19th Brazilian Congress of Thermal Sciences and Engineering
November 6th–10th, 2022, Bento Gonçalves - RS - Brazil

ENC-2022-0558
NUMERICAL SIMULATION OF THE GEOMETRICAL PARAMETERS INFLUENCE ON UNIFLOW CYCLONE RECIRCULATION ZONES

Arthur França Martins
Dener Silva de Almeida
Av. dos Portugueses, 1966 - Vila Bacanga, São Luís - MA, 65080-805
arthur.franca@discente.ufma.br
dener.almeida@ufma.br

Abstract. *There are records of the use of the cyclone in 1885 by DeLaval, when he demonstrated the separation of cream from milk. The operation of this device consists of the partial separation of heterogeneous mixtures through the generation of a turbulent flow. Cyclones are used with many industrial systems such as combustion involved low heat capacity fuels, with system that use large amounts of coal or when the fuel requires a long residence time to complete combustion and flue gas purification. Therefore, the purpose of this article is to present results of numerical simulations through CFD in the RANS approach, using the RNG κ-ε turbulence model with rotation flow dominance in order to evaluate the degree of influence of geometric and/or constructive parameters of the cyclone in the recirculation zone through velocity and pressure profiles. Results show that general trend is reduction of pressure and axial and tangential velocities values reduction with increasing of the cyclone length, that is, the distance to be covered by the fluid presents itself as the preponderant factor in the flow dynamics in the evaluated device.*

Keywords: *CFD, Velocity Profile, Pressure Profile*

1. INTRODUCTION

There are records that the use of the separation cyclone occurred for the first time in 1885 by DeLaval, when he demonstrated the separation of cream from milk (Gupta *et al.*). These devices are used in many industrial processes related to the energy and fuel sector such as the combustion of low heat capacity fuels, systems that use large amounts of coal or when the fuel requires a high residence time to complete combustion; typical dust separation processes related to air protection by flue gas filtering through soot removal; to technological processes such as drying, calcination and heating. Cyclones are simple structures, economical in terms of manufacture and operation, in addition to operating in a wide range of temperature and pressure conditions, in addition to requiring little or almost no maintenance due to the absence of moving parts (Noh *et al.*, 2018; Wasilewski and Brar, 2019). Basically, the main operation of the cyclone consists in the application of high acceleration of the fluid inlet, usually air and particulate matter, with the objective of achieving a partial separation of heterogeneous mixtures that present different densities.

The cylindrical shape of the cyclone, schematized in Fig. 1A, establishes a turbulent flow with swirl and the separation of the particles from the air stream occurs due to the difference in density between the particulate material and the air, so that the particulate material (usually solid) has a higher density than this gas. Due to the action of the centrifugal force, the larger particles move more quickly to the vicinity of the cyclone wall and are then later directed to the lower outlet, thus being collected. Smaller particles, in turn, move more slowly and are then caught in an upward flow (or inward flow, as will be seen) and are routed towards the upper outlet so that there is no particle collection. However, not all particulate matter is collected, thus resulting in reduced cyclone collection efficiency (Oh *et al.*, 2015; Xu *et al.*, 2016).

The cyclone schematized in Fig. 1A is the most used model in the industry. The main components of this device, which can be described by seven geometric parameters, are: height of the inlet section, h_A, width of the inlet section, b_A, so they are generally employed together and treated as the inlet area, A_t. This structure is in yellow; height of the cylindrical section, $l1$, in orange; total height of the cyclone, L, corresponding to the height of the orange section added to the height of the conical section, $l2$ in cyan; bottom outlet diameter, D_o (or particulate matter outlet), top outlet diameter, D_e (or purified air outlet), and vortex finder height, h, in green. Figure 1B presents the identification of the presented parameters. It is also noteworthy that these parameters are the main factors in determining the collection efficiency, pressure drop and diameter of the cylindrical section of the cyclone (Lucarelli *et al.*, 2019).

Figure 1A also presents the internal flow pattern of the cyclone. This pattern consists of a structure formed by two vortices called external and internal vortex. The outer vortex (or free vortex), in blue, is characterized by rotating through the cyclone walls towards the bottom exit, while the inner vortex (or forced vortex), in red, is rotating in the center of the device towards the top exit, so that the vortex structure resembles the Rankine vortex (model of a vortex developed in a viscous fluid) (Lucarelli *et al.*, 2019; Wasilewski and Brar, 2019).

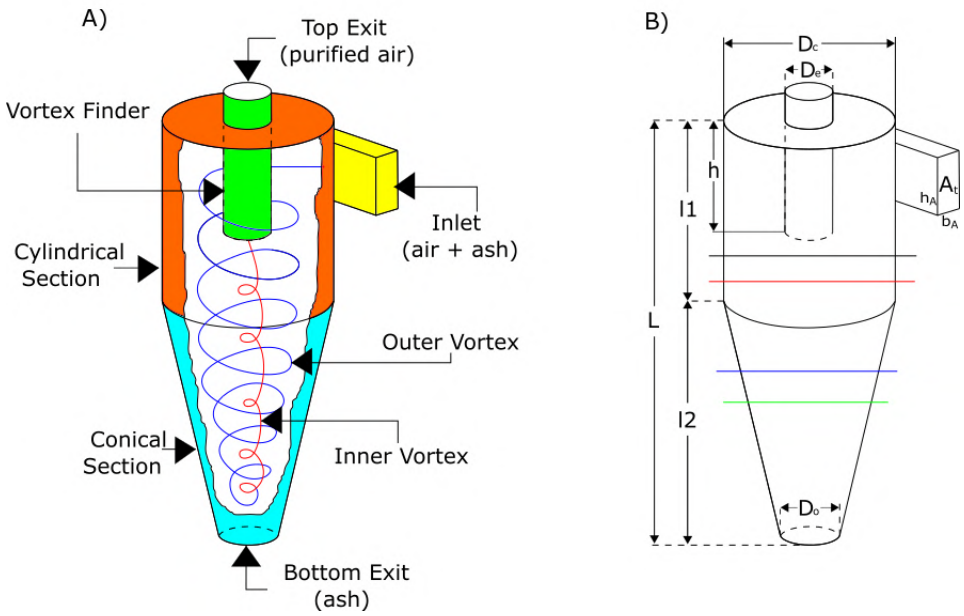

Figure 1. A) Components of the Cyclone. B) Cyclone Geometric Parameters

2. TURBULENCE MODEL

Recent works as Chauhan *et al.* (2022) has used the standard κ-ε model to analyze a cyclone. Pang *et al.* (2022), in turn, mention that the common turbulence models to describe a turbulent flow are: κ-ε standard, Reynolds Stress Model (RSM) and the large eddy simulation (LES). The author emphasizes that the performance of the κ-ε model is not satisfactory in conditions that present high swirl, while the LES model requires a high quality mesh, thus demanding high computational power. Finally, works performed by Hamdy *et al.* (2017) and Xu *et al.* (2016) cite the use of the κ-ε standard model and RNG κ-ε to simulate flow in cyclones as long as there is no high turbulence. Wasilewski (2017) compiles some works that employ RNG κ-ε in simulations, but points out that despite being a reliable model, there is a preference for the RSM model.

Given the above, the present work uses the κ-ε model based on RNG for numerical simulation. This turbulence model is composed of two equations in the form of Eq. (1) and Eq. (2). This model is derivide of Navier-Stokes equations through a technique called Renormalization or Renormalization Group (RNG). An analytical derivation results in a model with different constants than the κ-ε standard model, and additional terms and functions in transport equations for κ and ε. In general, the standard κ-ε , when compared to the κ-ε standard model presents greater precision for swirling flows due to the inclusion of the aforementioned terms.

$$\frac{\partial}{\partial t}(\rho\kappa) + \frac{\partial}{\partial x_i}(\rho\kappa u_i) = \frac{\partial}{\partial x_j}\left(\alpha_\kappa \mu_{eff}\frac{\partial \kappa}{\partial x_j}\right) + G_\kappa + G_b - \rho\varepsilon - Y_M + S_\kappa \tag{1}$$

$$\frac{\partial}{\partial t}(\rho\varepsilon) + \frac{\partial}{\partial x_i}(\rho\varepsilon u_i) = \frac{\partial}{\partial x_j}\left(\alpha_\varepsilon \mu_{eff}\frac{\partial \varepsilon}{\partial x_j}\right) + C_{1\varepsilon}\frac{\varepsilon}{\kappa}\left(G_\kappa + C_{3\varepsilon}G_b\right) - C^*_{2\varepsilon}\rho\frac{\varepsilon^2}{\kappa} \tag{2}$$

So that:

$$C^*_{2\varepsilon} = C_{2\varepsilon} + \frac{C_\mu \eta^3\left(1-\eta/\eta_0\right)}{1+\beta\eta^3} \tag{3}$$

Where:

$$\eta = \frac{S_\kappa}{\varepsilon} \tag{4}$$

So G_K represents the generation of kinetic turbulence energy due to average velocity gradients; G_b represents the generation of kinetic turbulence energy due to thrust; Y_M represents the contribution of fluctuating expansion to compressible turbulence to the overall rate of dissipation; the quantities α_κ and α_ε correspond to the Prandtl numbers for κ and ε, respectively. S_κ is a source term obtained according to user simulation. The Table 1 presents the constants used by turbulence model equations.

Table 1. Constants Used in the Simulation.

Constant	Value
C_μ	0.0845
$C_{1\varepsilon}$	1.4200
$C_{2\varepsilon}$	1.6800
η_0	4.3800
β	0.0120
Swirl Factor	0.0750

To predict the particle trajectory of the particulate matter discrete phase modelling was used (DPM). The Fluent employs it using the Euler-Lagrange method, thus making it possible to ignore the interaction between the particulate phase and the continuous phase (air) as long as the particle diameter is sufficiently small. Regarding the acting forces, it is known that particles in the cyclone flow field are mainly affected by the drag force and gravity, while the effect of other forces *e.g.* weight on the particles is small enough to be ignored without any detriment to the analysis. Generally, the amount of particles in the cyclone is typically small, corresponding to less than 10% of the volumetric fraction. It is possible to predict the trajectory of the particles through the solution of Newton's Second Law. Thus, the Eq. (5) and Eq. (6) represent the equations of motion for an individual particle (Pang *et al.*, 2022; Duan *et al.*, 2020).

$$\frac{dx_p}{dt} = u_p \tag{5}$$

$$\frac{du_p}{dt} = F_d\left(u - u_p\right) + \frac{g_x\left(\rho_p - \rho\right)}{\rho_p} \tag{6}$$

Where u_p, ρ_p e $F_d\left(u - u_p\right)$ represent, respectively, the velocity, density and the drag force, so it is defined as Eq. (7).

$$F_d = \frac{3\mu C_d Re_p}{4\rho_p {d_p}^2} \tag{7}$$

With C_d corresponds to the drag coefficient for spherical particles and its equation has the form of Eq. (8).

$$C_d = a_1 + \frac{a_2}{Re_p} + \frac{a_3}{{Re_p}^2} \tag{8}$$

Where a_1 , a_2 and a_3 correspond to constants for a wide range of the Relative Reynolds Number, Re_p , given by Morsi and Alexander (1972). The Relative Reynolds Number is expressed for Eq. (9).

$$Re_p = \rho d_p \frac{|u - u_p|}{\mu} \tag{9}$$

Also with regards to Fluent, it is important to note that DPM has its four settings for boundary conditions (input, output and wall), they are: reflect, trap, escape, wall jet and user defined. This work employs the reflect condition at the inlet and on the walls and escape at the upper and lower exits. The reflect condition, as the name implies, is the reflection of the particle when it touches the wall with a change in its moment defined by the coefficient of restitution (a dimensionless quantity that characterizes the different types of collision between two bodies); the escape condition, on the other hand, consists of changing the state of the particle as "escaped" when it encounters the surface in question, so that the trajectory calculations are terminated.

3. CONSTRUCTIVE ASPECTS AND METHODOLOGY

A wide variety of studies analyze the influence of geometric parameters on cyclone operation, such as: double cyclone design in which two cyclones were connected through a single box to evaluate their collection efficiency at different temperatures and flow rates (Smith *et al.*, 1982); cyclone cone length and changes in the inner and outer diameters (wall thickness) of the vortex locator (Saltzman and Hochstrasser, 1983; Elsayed and Lacor, 2013); cyclone length based on inlet

area, cylinder height and changes in flow (Iozia and Leith, 1989; Brar *et al.*, 2015); cyclone performance based on body diameter (cylindrical section) and vortex finder diameter ratios (Kim and Lee, 1990; Elsayed and Lacor, 2013); cyclone performance based on changes in cyclone height (Moore and McFarland, 1993; Hamdy *et al.*, 2017); cyclone efficiency based on bottom outlet diameter of the cone (Xiang *et al.*, 2001; Elsayed and Lacor, 2012); cyclone performance based on the use of one (Elsayed and Lacor, 2011) or two inlets (Lim *et al.*, 2003); comparison between collection efficiency and pressure drop between cyclones with various vortex finder designs (Lim *et al.*, 2004); and cyclone performance based on inlet angle (Bernardo *et al.*, 2006).

In view of the above, the present work aims to vary the following parameters present in Fig. 1B: inlet area A_t, outlet diameter D_o, diameter of the cylindrical section, D_c, and cyclone length, L. The analysis is performed by varying only one parameter at a time, while the others remain constant, and so on until all are checked. It is important to emphasize that the increment in L occurs through the increment of $l1$, that is, $l2$ remains constant. The Table 2 presents the dimensions for the reference cyclone, that is, any variation in the dimensions of the cyclone will be compared mainly with those of this model.

Table 2. Reference Cyclone Geometric Dimensions.

Variables	Values
D_c	100 mm
D_e	40 mm
D_o	30 mm
h	50 mm
$l1$	104 mm
$l2$	96 mm
L	200 mm
h_A	40 mm
b_A	25 mm
A_t	1000 mm^2

As mentioned in Topic 2, the RNG κ-ε model is far from reality for high swirl numbers, for this reason, this work adopts the Eq. (10) proposed by Gupta *et al.* for the Swirl number calculation. Despite presenting a simple formulation without considering flow velocity and other variables, it serves as a guide in order to guarantee the best representation of the flow through the results, like the example above (Table 2) that presents S = 0.942. The main objective is to keep S below 2. In fact, the average swirl number of this work corresponds to S = 1.047 $\pm$ 0.477 with maximum value corresponding to the condition where A_t = 500 mm^2, with S = 1.884.

$$S = \frac{\pi D_e D_o}{4 A_t} \tag{10}$$

ANSYS Fluent 2019 R3 was used for simulation and solve the cyclone flow field. The solution algorithm is the Semi-Implicit Method for Pressure Linked Equations (SIMPLE). The turbulence model, as already mentioned, is RNG κ-ε, with all spatial discretization based on second order under the steady-state condition. The iterative process has a stopping criterion of 1000 steps or a minimum residual of $1{\times}10^{-4}$. In terms of boundary conditions, air and ash (particulate matter) both enter at 10 m/s, with particles having a diameter of $1{\times}10^{-2}$ mm and ash flow rate is $1{\times}10^{-10}$ kg/s. The simulation was performed on a computer with an i5 8300H processor, GTX 1050 and 8 GB DDR4 memory.

4. RESULTS

The results obtained are presented in this section as well as their discussion. The colored bands refer to the data collection, with your position presented by Fig. 1B. The Figure 2 shows the influence of the inlet area (A_t) on the flow. It is noticed that the variation of the area, through increase/reduction of h_A, keeping the speed constant, so that each simulation has a different flow, causes the increase of the static pressure inside the cyclone. In addition, there is a closer approximation of surface A_t to the position point 60 mm Although there is an influence due to the way the results were taken, it appears that they present the same pattern obtained by Elsayed and Lacor (2011), that is, higher static pressure values are related to higher axial and tangential velocity, and that the tangential velocity presents greater variation than the axial velocity. It is noted that higher levels of pressure and axial velocity are located higher above the cyclone and, as it is directed to the lower outlet, there is a tendency to reduce their values while the tangential velocity presents the opposite behavior. The display of this behavior may be related to the fact that the blue and green lines are located on the conical part of the cyclone, corresponding to the 110 mm and 135 mm positions, that is, the tangential velocity increases due to the reduction of the area available for its development (closer to the wall).

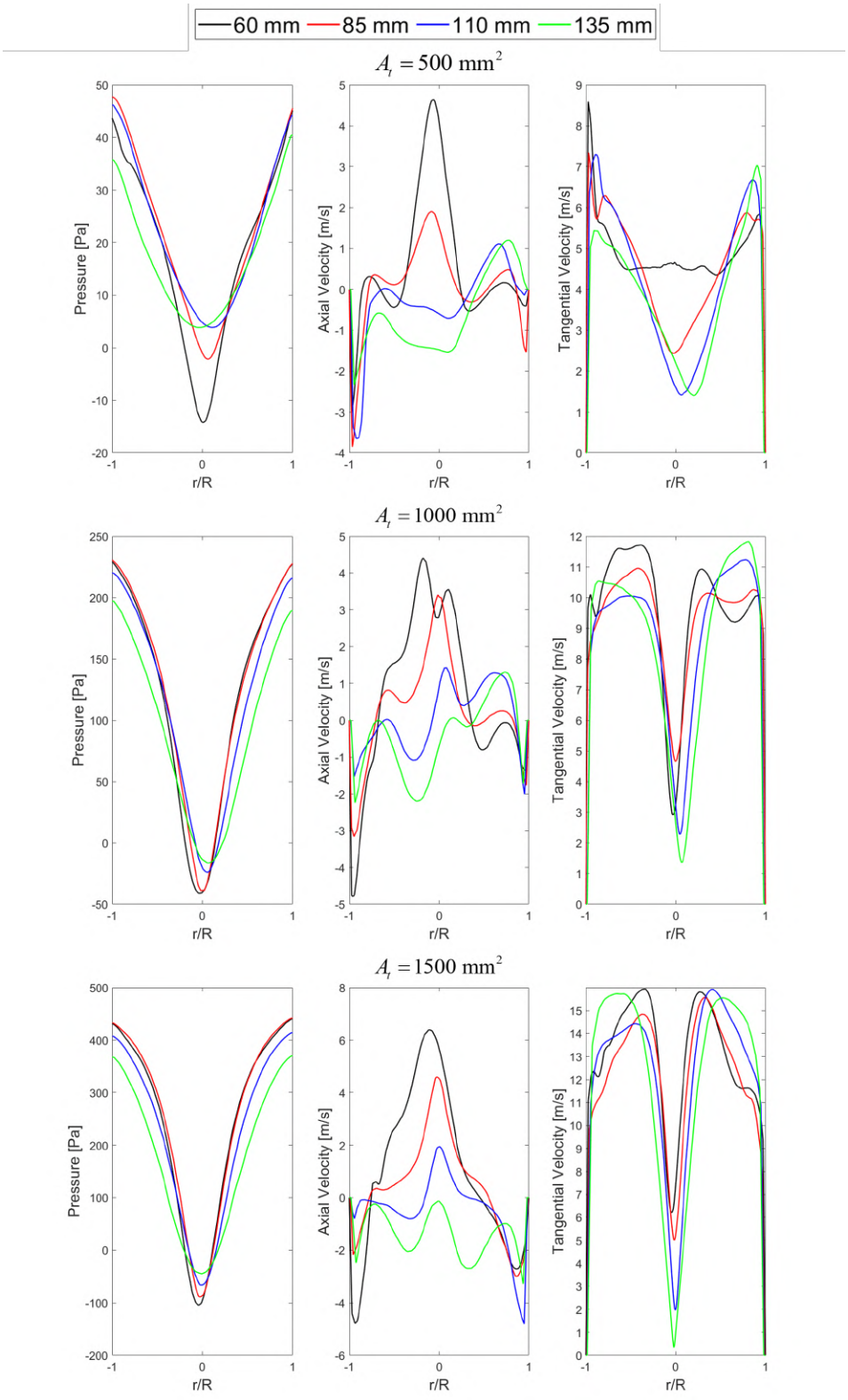

Figure 2. Influence of the Inlet Area

The Figure 3 shows the influence of the diameter on the flow (D_c). It is noticed that its increase causes a reduction of approximately 35 Pa for the maximum static pressure, 0.5 m/s for the maximum axial speed and 2 m/s for the maximum tangential speed. A larger diameter results in a greater distance traveled by the fluid in one turn of the cyclone, thus implying a reduction in its speed and, also, in energy due to friction with the cyclone wall and, for this reason, it is expected lower pressure and velocity as the diameter increases. For the pressure condition of 200 mm, the pressure profile presents a more accentuated reduction, that is, approximately 190 Pa against 35 Pa from 100 to 150 mm. In addition, the tangential velocity profile presents a different behavior from the others, for positions 60 and 85 mm, so that there is a

tendency to increase its value towards the central zone (near $r/R = 0$).

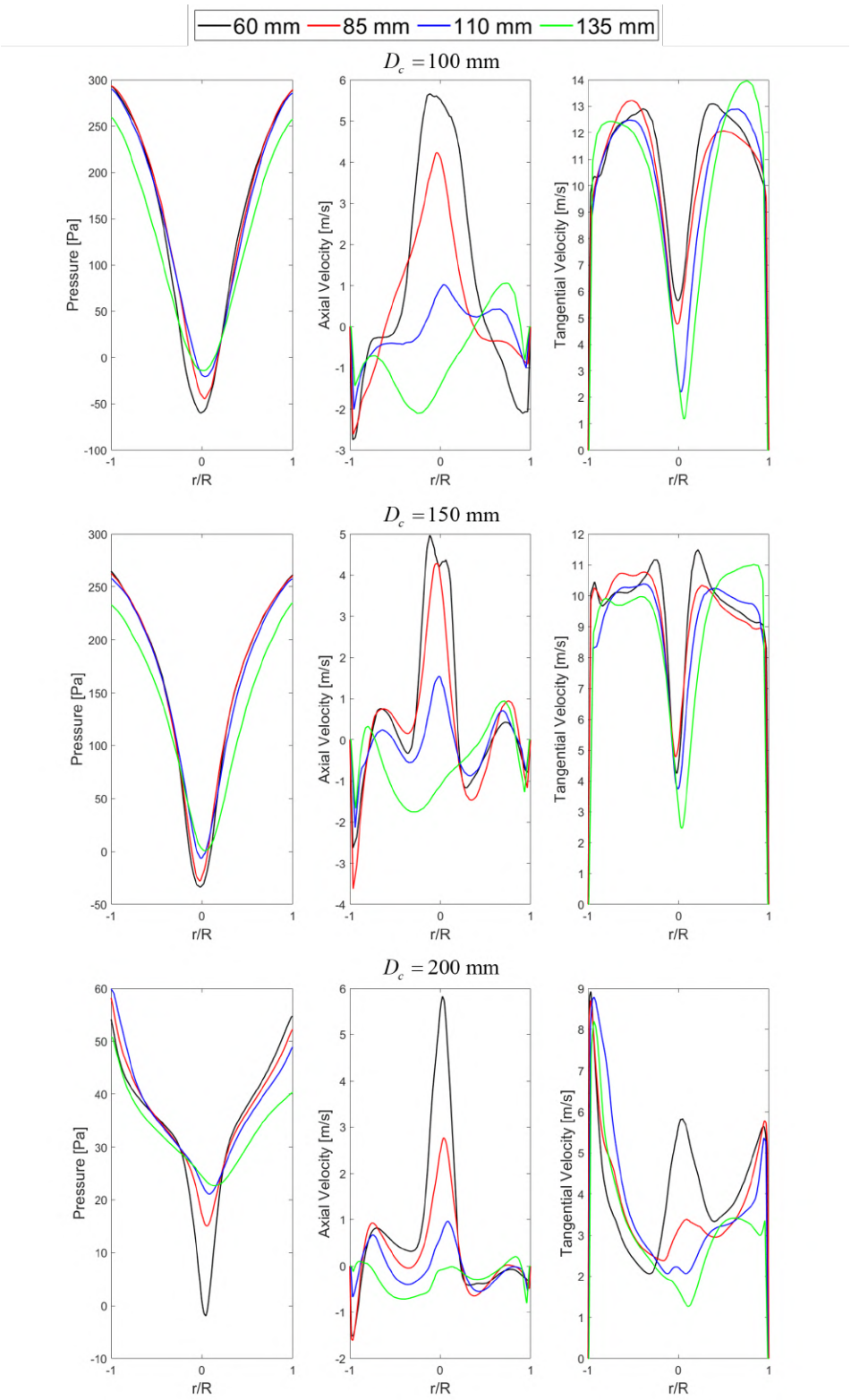

Figure 3. Influence of the Diameter of the Cylindrical Section.

Figure 4 shows the influence of the lower outlet diameter on the flow (D_o). It is noticed that its increase causes a reduction of pressure and axial and tangential velocities. This behavior was verified by Xiang *et al.* (2001) and later by Hsiao *et al.* (2015). For these authors, there is an acceleration of the flow due to the gradual reduction of the cross-sectional area since the reduction of the lower diameter keeping the length of the conic section, $l2$, constant reduces the angle of inclination of the cone. A smaller slope results in a smaller diameter section and therefore the fluid travels a

shorter distance per turn the smaller the outlet diameter. A shorter distance traveled is reflected in a lower loss of energy and speed, thus resulting in higher values for pressure and speed as the lower outlet diameter is reduced. Regarding the condition of D_o = 45 mm, it is noticed that there is no uniformity in the axial velocity profile, although it approaches 0.

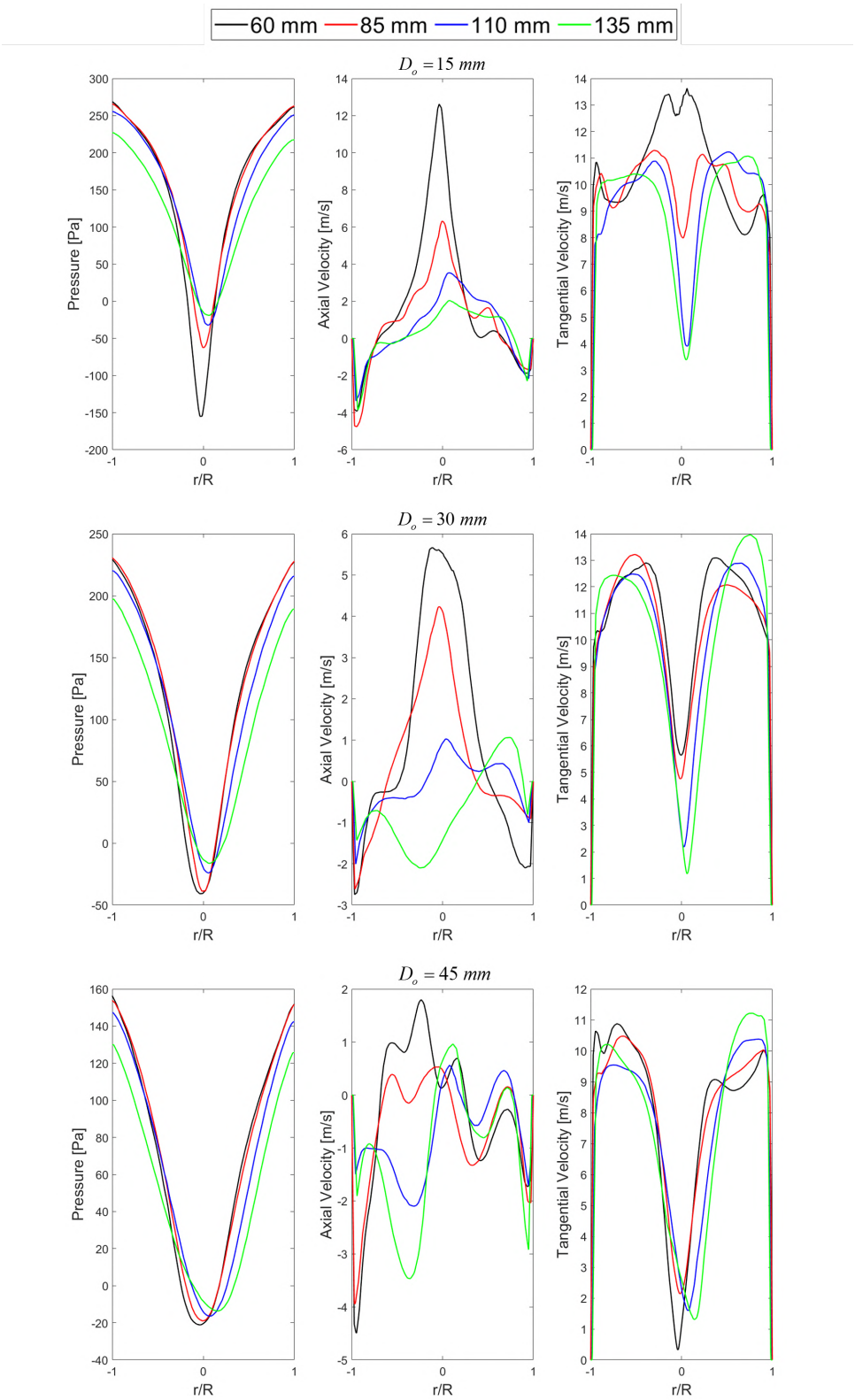

Figure 4. Influence of Bottom Outlet Diameter.

The Figure 5 shows the influence of length (L) on flow. The reduction of axial and tangential pressure and velocities is in accordance with Moore and Moore and McFarland (1993) and Hsiao *et al.* (2015). These authors classify this behavior

as the “pay” and the “gain” in the inertial separation process, that is, when L increases, there is an increase in the area of the inner wall of the cylindrical section to be traversed by the fluid, resulting in additional friction and , consequently, reduction of the intensity of the vortices resulting in reduced values for pressure and velocities (axial and tangential). However, the axial velocity profile does not reflect the expected result, so there is no significant variation for the 60 and 85 mm positions (cylindrical section) between the 200 and 250 mm conditions, with the 300 mm condition showing higher axial velocity, therefore, different from the expected, although there is a reduction for positions 110 mm and 135 mm, located in the conic section. Since there is no change in diameter in the cylindrical section, the velocity profile tends to remain constant.

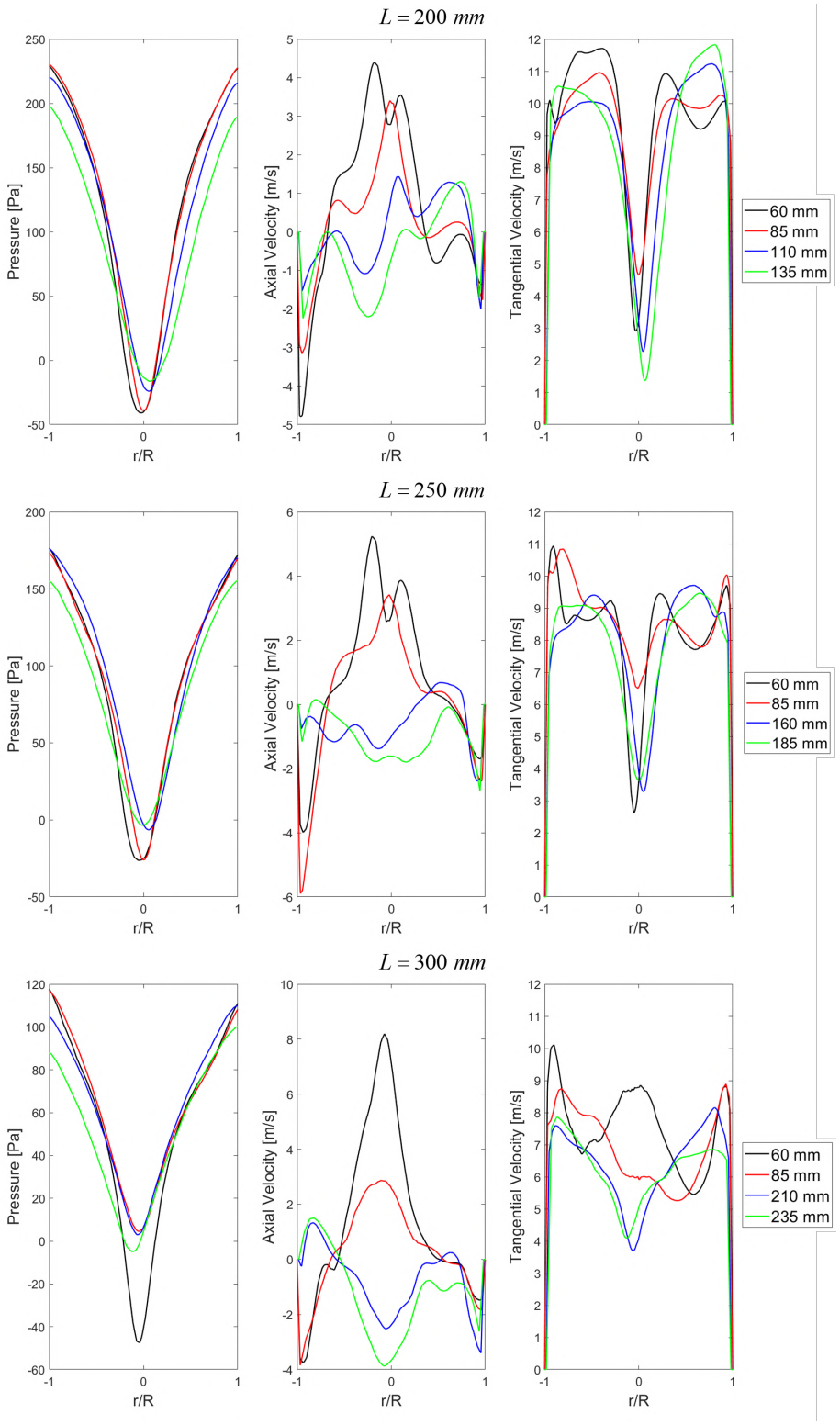

Figure 5. Influence of Cyclone Length.

5. CONCLUSIONS

The present work analyzed the influence of geometry on the recirculation zones formed in a single-stage cyclone with an inlet through velocity and pressure profiles. Among the parameters evaluated (A_t, D_o, D_c and L), the length L implies a reduction in amplitude in the analyzed profiles. In this way, the distance to be covered by the fluid is presented as the preponderant parameter in the flow behavior along the cyclone, while the others provide flows with similar characteristics.

Furthermore, the model-based simulation RNG κ-ε provided the attainment of profiles with behaviors predicted by the literature. Therefore, such a turbulence model is satisfactory for a qualitative analysis, although there is some departure from reality *e.g.* axial velocity profiles, and for detailed analysis aiming at more realistic values, it is recommended to use more accurate models, such as those based on LES or RSM.

6. REFERENCES

Bernardo, S., Mori, M., Peres, A. and Dionisio, R., 2006. "3-d computational fluid dynamics for gas and gas-particle flows in a cyclone with different inlet section angles". *Powder Technology*, Vol. 162, No. 3, pp. 190–200. ISSN 0032-5910. doi:https://doi.org/10.1016/j.powtec.2005.11.007.

Brar, L.S., Sharma, R. and Elsayed, K., 2015. "The effect of the cyclone length on the performance of stairmand high-efficiency cyclone". *Powder Technology*, Vol. 286, pp. 668–677. ISSN 0032-5910. doi: https://doi.org/10.1016/j.powtec.2015.09.003.

Chauhan, J., Salvi, B.L., Khidiya, M.S. and Agrawal, C., 2022. "Computational fluid dynamic analysis of cyclone separator for flue gas cleaning by using standard k-epsilon model". In P. Verma, O.D. Samuel, T.N. Verma and G. Dwivedi, eds., *Advancement in Materials, Manufacturing and Energy Engineering, Vol. II*. Springer Nature Singapore, Singapore, pp. 25–34. ISBN 978-981-16-8341-1.

Duan, J., Gao, S., Lu, Y., Wang, W., Zhang, P. and Li, C., 2020. "Study and optimization of flow field in a novel cyclone separator with inner cylinder". *Advanced Powder Technology*, Vol. 31, No. 10, pp. 4166–4179. ISSN 0921-8831. doi:https://doi.org/10.1016/j.apt.2020.08.020.

Elsayed, K. and Lacor, C., 2011. "The effect of cyclone inlet dimensions on the flow pattern and performance". *Applied Mathematical Modelling*, Vol. 35, No. 4, pp. 1952–1968. ISSN 0307-904X. doi: https://doi.org/10.1016/j.apm.2010.11.007.

Elsayed, K. and Lacor, C., 2012. "The effect of the dust outlet geometry on the performance and hydrodynamics of gas cyclones". *Computers Fluids*, Vol. 68, pp. 134–147. ISSN 0045-7930. doi: https://doi.org/10.1016/j.compfluid.2012.07.029.

Elsayed, K. and Lacor, C., 2013. "The effect of cyclone vortex finder dimensions on the flow pattern and performance using les". *Computers Fluids*, Vol. 71, pp. 224–239. ISSN 0045-7930. doi: https://doi.org/10.1016/j.compfluid.2012.09.027.

Gupta, A., Lilley, D. and Syred, N., ???? *Swirl Flows*. Energy and engineering science series. Abacus Press. ISBN 9780856261756.

Hamdy, O., Bassily, M.A., El-Batsh, H.M. and Mekhail, T.A., 2017. "Numerical study of the effect of changing the cyclone cone length on the gas flow field". *Applied Mathematical Modelling*, Vol. 46, pp. 81–97. ISSN 0307-904X. doi:https://doi.org/10.1016/j.apm.2017.01.069.

Hsiao, T.C., Huang, S.H., Hsu, C.W., Chen, C.C. and Chang, P.K., 2015. "Effects of the geometric configuration on cyclone performance". *Journal of Aerosol Science*, Vol. 86, pp. 1–12. ISSN 0021-8502. doi: https://doi.org/10.1016/j.jaerosci.2015.03.005.

Iozia, D.L. and Leith, D., 1989. "Effect of cyclone dimensions on gas flow pattern and collection efficiency". *Aerosol Science and Technology*, Vol. 10, No. 3, pp. 491–500. doi:10.1080/02786828908959289.

Kim, J.C. and Lee, K.W., 1990. "Experimental study of particle collection by small cyclones". *Aerosol Science and Technology*, Vol. 12, No. 4, pp. 1003–1015. doi:10.1080/02786829008959410.

Lim, K., Kim, H. and Lee, K., 2004. "Characteristics of the collection efficiency for a cyclone with different vortex finder shapes". *Journal of Aerosol Science*, Vol. 35, No. 6, pp. 743–754. ISSN 0021-8502. doi: https://doi.org/10.1016/j.jaerosci.2003.12.002.

Lim, K., Kwon, S. and Lee, K., 2003. "Characteristics of the collection efficiency for a double inlet cyclone with clean air". *Journal of Aerosol Science*, Vol. 34, No. 8, pp. 1085–1095. ISSN 0021-8502. doi:https://doi.org/10.1016/S0021-8502(03)00079-X.

Lucarelli, N., Eckman, E. and Disotell, K., 2019. "Cfd analysis of cyclone separator flow field in advance of experiment". pp. 1–12. doi:10.2514/6.2019-3496.

Moore, M.E. and McFarland, A.R., 1993. "Performance modeling of single-inlet aerosol sampling cyclones". *Environmental Science & Technology*, Vol. 27, No. 9, pp. 1842–1848. doi:https://doi.org/10.1021/es00046a012.

Morsi, S.A. and Alexander, A.J., 1972. "An investigation of particle trajectories in two-phase flow systems". *Journal of Fluid Mechanics*, Vol. 55, No. 2, p. 193–208. doi:https://doi.org/10.1017/S0022112072001806.

Noh, S.Y., Heo, J.E., Woo, S.H., Kim, S.J., Ock, M.H., Kim, Y.J. and Yook, S.J., 2018. "Performance improvement of a cyclone separator using multiple subsidiary cyclones". *Powder Technology*, Vol. 338, pp. 145–152. ISSN 0032-5910. doi:https://doi.org/10.1016/j.powtec.2018.07.015.

Oh, J., Choi, S. and Kim, J., 2015. "Numerical simulation of an internal flow field in a uniflow cyclone separator". *Powder Technology*, Vol. 274, pp. 135–145. ISSN 0032-5910. doi:https://doi.org/10.1016/j.powtec.2015.01.015.

Pang, X., Wang, C., Yang, W., Fan, H., Zhong, S., Zheng, W., Zou, H. and Chen, S., 2022. "Numerical simulation of a cyclone separator to recycle the active components of waste lithium batteries". *Engineering Applications of Computational Fluid Mechanics*, Vol. 16, No. 1, pp. 937–951. doi:10.1080/19942060.2022.2053343.

Saltzman, B.E. and Hochstrasser, J.M., 1983. "Design and performance of miniature cyclones for respirable aerosol sampling". *Environmental Science & Technology*, Vol. 17, No. 7, pp. 418–424. doi:https://doi.org/10.1021/es00113a011.

Smith, W., Cushing, K., Wilson, R. and Harris, D., 1982. "Cyclone samplers for measuring the concentration of inhalable particles in process streams". *Journal of Aerosol Science*, Vol. 13, No. 3, pp. 259–267. ISSN 0021-8502. doi:https://doi.org/10.1016/0021-8502(82)90067-2.

Wasilewski, M., 2017. "Analysis of the effect of counter-cone location on cyclone separator efficiency". *Separation and Purification Technology*, Vol. 179, pp. 236–247. ISSN 1383-5866. doi:https://doi.org/10.1016/j.seppur.2017.02.012.

Wasilewski, M. and Brar, L.S., 2019. "Effect of the inlet duct angle on the performance of cyclone separators". *Separation and Purification Technology*, Vol. 213, pp. 19–33. ISSN 1383-5866. doi:https://doi.org/10.1016/j.seppur.2018.12.023.

Xiang, R., Park, S. and Lee, K., 2001. "Effects of cone dimension on cyclone performance". *Journal of Aerosol Science*, Vol. 32, No. 4, pp. 549–561. ISSN 0021-8502. doi:https://doi.org/10.1016/S0021-8502(00)00094-X.

Xu, W., Li, Q., Wang, J. and Jin, Y., 2016. "Performance evaluation of a new cyclone separator – part ii simulation results". *Separation and Purification Technology*, Vol. 160, pp. 112–116. ISSN 1383-5866. doi:https://doi.org/10.1016/j.seppur.2016.01.012.

7. RESPONSIBILITY NOTICE

The authors are solely responsible for the printed material included in this paper.